Sensitivity Analysis for a PEM Fuel Cell Model aimed to Optimization

Sensitivity Analysis for a PEM Fuel Cell Model aimed to Optimization

E. TESTA, P. MAGGIORE, L. PACE and M. D. L. DALLA VEDOVA
Department of Mechanical and Aerospace Engineering
Politecnico di Torino
Corso Duca degli Abruzzi 24 – 10129, Turin
ITALY
matteo.dallavedova@polito.it

Abstract: - The amount of current density produced by the stack is the key performance parameter for a fuel cell, given a well-defined quantity of reactants flowing through it. A Proton Exchange Membrane fuel cell (PEMFC) distributed parameters model is considered with all the aspects influencing the cell behavior. A sensitivity analysis is performed through a Monte Carlo Simulation to assess the impact on performances of key parameters. The Pareto plot obtained from such analysis allow to operate design variables reduction, aimed to those parameters that show small impact, so to decrease the problem complexity through an increased orthogonality of the input design matrix. The target of the activity is to obtain and validate a method able to reduce the time needed for a complete simulation, so to be able to realize an effective multi-disciplinary design optimization.

Key-Words: - MDO, PEM fuel cell, Surrogate model, Numerical Simulation

1 Introduction

Proton Exchange Membrane Fuel Cell (PEMFC) is one of the main technologies in the field of environmentally sustainable energy; as such, it is gaining increasing interest in the automotive and aerospace industry. As shown in Figure 1, PEMFCs typically uses a water-based, acidic polymer membrane as its electrolyte, with platinum-based electrodes that split the hydrogen into positive ions (H+, protons) and negative electrons. H+ ions pass through the membrane to the cathode to combine with oxygen to produce water. Electrons must pass round an external circuit creating a current to rejoin H+ ions on the cathode. PEMFC cells operate at relatively low temperatures (typically below 100 °C) and can tailor electrical output to meet dynamic power requirements; due to the relatively low temperatures and the use of precious metal-based electrodes, these cells must operate on pure hydrogen. Hydrogen fuel is processed at the anode where electrons are separated from protons on the surface of a platinum-based catalyst. The protons pass through the membrane to the cathode side of the cell while the electrons travel in an external circuit, generating the electrical output of the cell. On the cathode side, another platinum electrode combines protons and electrons with oxygen to produce water, which is expelled as the only by-product; oxygen can be provided in a purified form, or extracted at the electrode from atmospheric air.

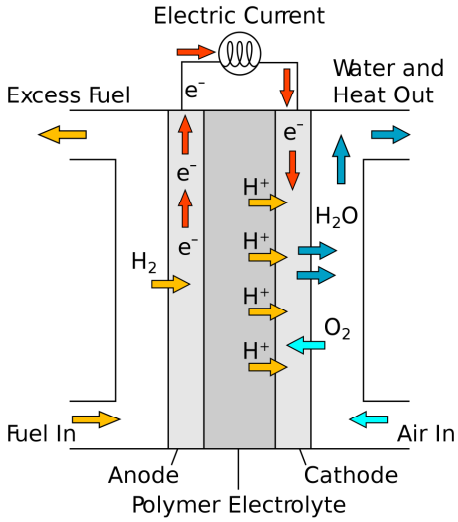

Fig. 1: Schematic representation of a PEMFC.

To assess the behavior of the system since the design phase, it is necessary to correlate the associated numerical simulation models (several Computational Fluid Dynamics - CFD - models have been realized and are available in literature) with experimental data, so to obtain a characterization and validation. Improvements in computer science technologies and the consequent reduction of computational time permitted some CFD models to gain interest and diffusion during the last decade, enabling even more robust and complex models.

The use of numerical modelling allows a great flexibility in the design and analysis of fuel cells [1]. The numerical model developed by Dutta, Shimpalee and Van Zee in 2000 and 2001 [2, 3] used semi-empirical relations for the fuel cell membrane characterization taken by Springer et al. [4]. All of the other CFD models developed further improved the detail of the phenomenological aspects involved in a PEM fuel cell operation [5, 6]. Several reviews on models developed for PEMFC are available in literature [7-13].

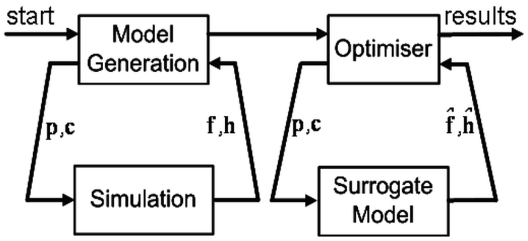

Fig. 2: Logical scheme of the sequential approach used in this study. The "model generation" and the "simulation" blocks refers to the "real model" on which the surrogate model is built for the target optimization. The sensitivity analysis and the corresponding DoE are performed at the "simulation" block level.

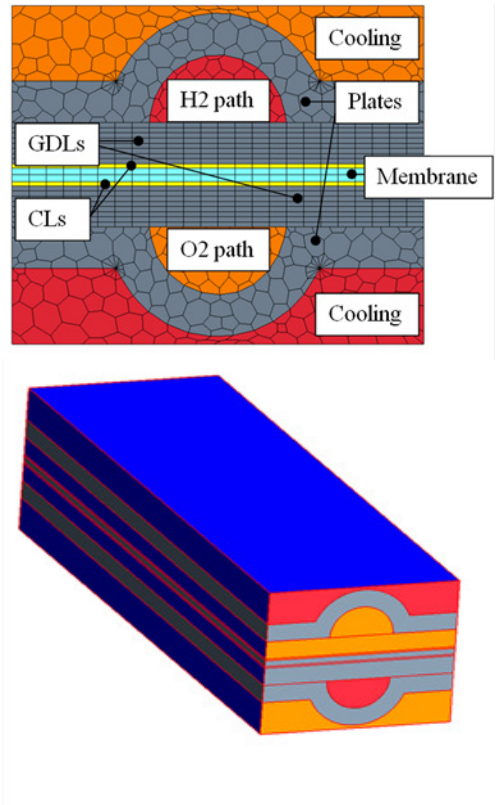

Fig. 3: Geometrical layout of the fuel cell portion simulated. At the bottom, the entire domain of about 3 x 2.8 x 10 mm is shown. Polyhedral cells are used for the meshing generation. On the upside, the components of the simulated cell are shown. CLs are the catalyst layers; GDL is the Gas Diffusion Layer.

The first improvements in the models were the adoption of a multi-phase flow instead of a simpler mono-phase flow – where both presence and effects of liquid water were not taken into account as presented in Siegel et al. [14], non-isothermal equations and the simulation of a 3D domain [15, 16] instead of a simpler 2D domain, so to consider also the geometrical effects; consequences of two-phases flow are shown in [17]. At present, the most detailed models implement 3D geometries of a complete fuel cell, with non-isothermal and multi-phase flows, capillary pressure, 3D electrochemical and membrane models, and a deeply detailed formulation of the porous media [18] and catalyst layers behaviour. A CFD model of a PEM fuel cell is considered in this paper as a test bench [19]. This model was developed to simulate a 3D complete fuel cell channel, and considering non-isothermal equations, steady-state conditions, compression effects and implementing a pseudo bi-phase flow instead of a fully two-phase flow solution [20]. One of the most important points is to identify the parameters sensibly affecting the performance, excluding the less relevant ones, to reduce the number of variables to be considered during the successive analyses. The goal of this paper is to provide a sensitivity analysis able to outline the best suitable approach to perform an MDO process of a PEM fuel cell through a surrogate model, starting from its distributed parameters model, as shown in Figure 2. To understand the needs of the MDO side, a review of the applicable methods has been done. Considering the available literature, dealing mainly with sensitivity analyses, a model validation approach can be found in Min et al. [21]. Guvelioglu and Stenger [22] report the influence of some cell operating parameters on the current density. Secanell et al. [23] set up an optimization tool for the Membrane Electrode Assembly (MEA) of a PEM fuel cell together with a sensitivity analysis. The variation of the cell output given by the gas diffusion layer parameters are investigated also in Pourmahmoud et al. [24] and in Ahmadi et al. [25]. Kim and Sun [26] dealt with the optimization of the flow channels topology. A review of methods dedicated to numerical optimization processes is provided by Secannell et al. [27]; the approaches provided in Mukhtar et al. [28], Rubinstein & Kroese [29] and Deb [30] are considered to be particularly relevant. The fuel cell model used here is referred to [31] and validated with empirical values given in literature. The model here used considers all the most important physical aspects involved, and it is based on previous CFD PEM fuel cell models available in literature.

Its geometrical layout is shown in Figure 3. The Membrane Electrode Assembly is composed of two 0.3 mm Gas Diffusion Layers (GDL), a couple of 30µm catalyst layers and a 0.1mm thick Proton Exchange Membrane. The mesh is realized through 38400 hexahedral cells, the GDLs are made up of eight layers (30720 cells), while the Catalyst Layer is constituted by a single layer cells (3840 cells), operating only as an interface to localize chemical reactions. The PEM is composed of two layers (3840 cells) with the only role to pass thermal fluxes data from side to side and to avoid reactants mixing. The hexahedral shape has been chosen for its rapidity in meshing, calculus, and with the aim to simplify the electrochemical field solution. The other fluid zones, i.e. the reactants channels and the water cooling channels, and the solid bipolar plates are constituted by polyhedral elements with variable face numbers and conformal mesh at the interfaces. There are in total 22193 cells (3428 cells for channels, 5601 for plates and 4484 for water channels); this kind of cells are usually not adopted in fuel cells CFD simulations available in literature, where the classic hexahedral cells are usually employed; polyhedral cells constitute a valid alternative, being capable to better cope with flux irregularities and, at the same time, preserving good mesh quality even with coarse discretization. Boundary layer is not present in the gas and water channels, since pressure drops across a 1 cm length cell can be neglected. The model is implemented in CD-adapco Star-CCM+ software environment, with an extensive use of user-defined functions. The main characteristics of this model are a 3D simulation domain comprising both fluid and solid regions, a steady-state solution, the adoption of a multicomponent gas and non-isothermal conditions. The flow considered is single-phase. The basic equations for the computation of the fluid flow, the diffusivity of the reactants and the ionic conductivity of the membrane are the same that can be found in [24]. The electrochemical model uses the standard electrochemical laws implemented in [20]. The main difference consists in using an arcsine function instead of a logarithmic one for the electrochemical activation losses. The presence of liquid water and its effects on the cell performance (occlusion of catalyst reaction sites and flooding phenomena) are considered despite the single-phase presence. This approach was based on Dawes et al. [20]. The liquid water presence and quantity is calculated from the value of relative and absolute humidity, and the electrochemical and fluid-dynamics performances are scaled (degraded) based on liquid water calculated in each cell of the computational domain. The level of liquid water presence is quantified with the saturation (s, dimensionless) value [18]. The phase-change of vapor into liquid water is considered (imposing gas sinks) and modelled as in the ANSYS FLUENT fuel cell modules manual [32]. The geometrical domain simulated comprised only a single channel of the cell to limit the computational cost. The presence of the other fuel cell channels can be also simulated varying the starting value of the saturation variable. In this model, the simulation comprises not only the membrane electrode assembly (membrane, catalyst layers and gas diffusion layers), but also the fluid channels, the solid bipolar plates (affecting the heat transfer [33]) and the cooling water flowing on the opposite side of the plates. Together with the indirect liquid water presence simulation, the other main aspect differentiating this model from others is the reduction in the porosity of the gas diffusion layers given by the clamping pressure of the stack, as discussed in [15]

2 Methodology

A design space evaluation was performed considering the performance of the fuel cell from a fluid dynamics and electrochemical point of view. A set of parameters was selected and then split into two main sets.

The boundary conditions values (first set of design variables), also defined "uncontrollable input noises" or "noise factors" [34, 35], are:

Cathode exchange current density, i_{0c}: the exchange current density is an important electrochemical parameter related to the kinetics of the chemical reactions. This variable depends upon many physical and electro-chemical factors, as the noble metal particles used, their shape and distribution over the catalytic surfaces and the micro-structure of the supporting surfaces. In the model, it is defined for both the cathode and the anode sides. This variable is usually measured in A/cm^2. The higher its value, the faster the chemical reactions. A quicker chemical reaction has the direct effect of lowering the detrimental voltage losses, since it implies a lower amount of energy absorbed by the reaction itself (in the form of a voltage loss), improving the power output. The cathode exchange current density for a PEM fuel cell is usually in the range of 0.01-5 A/cm^2, while the anodic reaction exhibits an exchange current density of about 1000-3000 A/cm^2 [3]. From an electrochemical point of view, the cathode exchange current density produces the well-identifiable initial voltage drop at very low current densities. The initial voltage drop

translates the whole fuel cell polarization curve into lower voltage values, i.e. it reduces the overall cell efficiency. Therefore, this control factor is expected to have a strong influence on the cell performance.

Anode exchange current density, i_{0a}.

Condensation rate, r_{cond}. The condensation rate is a gain factor (measured in 1/s) directly related to the kinetics of water vapor condensation into liquid form. This value is usually defined in the range of 100-200 1/s by commercial software (e.g. ANSYS Fluent [32]) for the simulation of generic multiphase flows contemplating a transition from vapor to liquid form. In the Fluent PEMFC model this value is set to 100/s.

Saturation coefficient, sat_{rate}: this parameter is another gain factor used in the definition of the saturation variable (s), implemented for simulating major or minor quantities of liquid water presence inside the porous media. It is defined as the ratio of volume occupied by liquid water divided by void volume available within the dry porous structure of the Gas Diffusion Layer (GDL). When simulating a portion of fuel cell, it allows the user to take into account the presence of the whole cell, i.e. the liquid water produced by the part of the cell that is not really considered in the simulation can be modelled by assuming a suitable value of the sat_{rate}. The effects of the presence of liquid water are here considered.

On the other hand, the *tuning parameters*, also defined "*control factors*", are summarized below:

Anode inlet gas temperature, T_a: the temperature of the gas mixture entering at the hydrogen side.

Anode inlet relative humidity, Rh_a: the relative humidity of the gas mixture entering the cell at the hydrogen side. In case of PEMFCs, the polymer membrane requires high level of humidity to operate properly as electrolytic element of the cell. Despite the cell produces liquid water as a chemical by-product at the cathode side, it is often not sufficient to guarantee a proper membrane operation [36, 37]. For this reason, it is often required to inject hydrogen at a high level of humidification for medium-large fuel cell stack.

Cathode inlet gas temperature, T_c: the temperature of the gas mixture (H_2 and H_2O) entering the cell at the oxygen side.

Cathode inlet relative humidity, Rh_c: the relative humidity of the gas mixture (O_2, N_2 and H_2O) entering the cell at the oxygen side.

Compression (of the GDL), compr: the effects of the torque applied to clamp the stack. The clamping force, required to prevent reactants leakage and a good contact between the electric conductive parts, has the counteracting effect of reducing the porosity of the gas diffusion layers, directly reducing the void volume available to the reactants. In the model, the gas permeability and diffusivity are reduced as function of the dry porosity of the GDL influenced by the stack clamping pressure. The reduction in electrical contact resistance between catalyst, GDL and electrodes given in case of stronger clamping forces are not considered in this model.

Geometrical parameters (gas channel width, gas channel length, etc.) are defined as "*controllable inputs*" since their uncertainty level can be controlled during the manufacturing process [5, 34]. They are not involved in the presented sensitivity analysis, since this study is done for a fixed fuel cell geometry.

The design space evaluation is often performed through the use of a Design of Experiments (DoE) technique. The advantage of using a DoE consists in a maximum amount of knowledge gained with a minimum expense of numerical trials. Due to the fact that analysis processes are often time consuming, an efficient exploration of the entire design space requires a systematic samples distribution. The objective is to get many representative details of the correlation between system response and design parameters, while at the same time minimizing the number of design evaluations [29, 34- 40]. Several strategies can be used to generate appropriate samples [14, 41]: Monte Carlo Simulation (MCS), Latin Hypercube Sampling (LHS), Optimal Latin Hypercube Sampling (OLHS) and Factorial Designs. According to literature references [40] and thanks to the low complexity of this model, the MCS approach is used here. For the purposes of this work, a Sample Random Sampling (SRS) technique is used [28, 30, 40], consisting in generating random values according to a certain distribution.

This technique has been preferred by the authors because it gives an absolutely random distribution. As a result, this technique generates random sample points instead of dividing the distribution into N intervals of equal probability. The major drawback of this approach is that the design points may be clustered in some regions of the design space whereas other parts could be almost unexplored.

To avoid this situation, (i.e., to achieve an almost even distribution of the design points), a significant number of simulations is required. So, this method should be used just in case of fast running analyses, while other algorithms should be considered for a complete covering of the design space.

A uniform Probability Density Function (PDF) – instead of a common Normal one, is adopted to model the random behavior, obtaining in this way a

matrix containing the generated values of input parameters. The choice of a uniform PDF is motivated by the fact that a sensitivity analysis is performed evaluating all the values the parameters could assume, without having values with different likelihood, in a range included between upper and lower bounds. The PDF is also allowed thanks to the absence of geometrical parameters considered.

Moreover, selected DoE techniques have to ensure the orthogonality of the generated matrix of design variables (i.e. its transpose is equal to its inverse) to ensure a good fit of meta-models [41]. An advantage of using orthogonal design variables as a basis for fitting data is that the inputs can be decoupled in the analysis of variance [27].

Orthogonality implies the estimates of the effects are uncorrelated, where any pair of independent variables is linearly independent. The most familiar measure of dependence between two quantities is the Pearson product-moment correlation coefficient ($\rho_{X,Y}$) also called Pearson's correlation [42, 43]. It is obtained by dividing the covariance of the two variables by the product of their standard deviations.

$$\rho_{X,Y} = \frac{\operatorname{cov}(X,Y)}{\sigma_X \sigma_Y} = \frac{E[(X-\mu_X)(Y-\mu_Y)]}{\sigma_X \sigma_Y} \quad (1)$$

The larger the correlation, the less independent the parameters and the less orthogonal the design matrix is. If the design matrix is not orthogonal, a coupling exists in the matrix, so that the interaction effects of independent variables are not distinguishable [44]. As a second step, a sensitivity analysis was done to evaluate which parameters have the major weight on the system response. This was done thanks to the *iSight* software, providing some useful visual tools. After performing the DoE, a 2nd order polynomial was chosen as approximated function. The function fits the responses on a discrete set of samples after calculating the function coefficients thanks to the least square method. The unknown model function can be approximated by a 2nd order Taylor series. Moreover, it is possible to use one-dimensional cuts through the response surface to quantify the influence of the parameters distinctly. The influence of the design parameters is displayed in a classic Pareto plot, where positive effects on the responses are marked in blue, whereas negative effects are colored in red. The last presented representation is more direct than other graphic results, giving the designer a useful tool to better understand which design parameters could be neglected because of their poor effect on global performances [21].

According to common techniques of robust design [34], the two sets of parameters are kept separated and two different sensitivity analyses are done to evaluate the influence of each set on the outputs separately. Furthermore, an overall analysis considering all of the parameters at the same time would require a definitely higher number of trials, determining an unacceptable amount of time spent in simulating, as the noise and control factors could sensibly influence each other.

Therefore, for the purposes of the present work, two different analyses gave a satisfactory result at a feasible computational cost. The reference output monitored is the current density: at a fixed user defined operating voltage, the higher its value, the higher the power output available from the fuel cell. Considering the number of trials to be simulated and the splitting of the sensitivity analysis into two different ones, an amount of 100 simulations has been chosen as a compromise between computational cost and sufficiently reliable preliminary results.

The sensitivity analysis tool provides different graphs and post-processing features. During a preliminary analysis, the most meaningful charts are the scatter plots and the Pareto plots, presented later in the text. Considering the operating conditions at which the cell is investigated, the authors decided to start with the analysis of possible flooding (at low voltage and high current density), opting for 0.2 V.

Only one single point of the polarization curve is analyzed, being anyway one of the most representative ones, where the cell is particularly sensible to change in performances. Also a validation of the approach based on the simulation of a single point could better test the goodness of the methodology.

3 Results and Discussions

After the run completion, the first step of the design space evaluation consisted in determining the level of orthogonality of the input variables.

Two different correlation matrices are presented for both noise and control factors (defined Table 1 and Table 2, respectively), obtained considering data related to the present case study.

As it can be seen, both noise and control factors present a very low correlation. These results are important because, as stated before, this is a useful preliminary step to get a good fitting response of the meta-model, avoiding to get confounding behaviors.

If the correlation factor is not close to a zero value, there is some level of confounding of the independent variables and this would affect the ability to estimate the source of variability in the system response and the associated model coefficients [45]. The ability of the surrogate model to approximate the reality in a better way is given by the lack of void spaces in the design space. If void spaces are present, the surrogate model would consider regions not covered by data, making the model error excessive.

	i_{0a}	i_{0c}	r_{cond}	sat_{rate}
i_{0a}	1	-0.127	-0.114	0.0725
i_{0c}	-0.127	1	0.124	-0.029
r_{cond}	-0.114	0.124	1	-0.066
sat_{rate}	0.0725	-0.029	-0.066	1

Tab. 1: Noise factors correlation matrix, showing the mutual influence of each variable on the others. 1 indicates perfect match and 0 complete non-correlation.

	T_a	Rh_a	T_c	Rh_c	*Compr*
T_a	1	-0.082	0.238	0.102	0.0064
Rh_a	-0.082	1	0.026	-0.091	-0.062
T_c	0.238	0.026	1	0.12	0.11
Rh_c	0.102	-0.091	0.12	1	0.0352
Compr	0.0064	-0.062	0.11	0.0352	1

Tab. 2: Control factors correlation matrix, presenting the mutual influence of each variable on the others. 1 indicates perfect match and 0 complete non-correlation.

Figure 4 shows the scatter plots originating from the present analysis on control factors. Examining such plots, the most interesting result is the direct proportionality between the current density and anode relative humidity. The Pareto plot that is obtained (shown in Figure 6, top part) clearly shows the relative weight of each of the selected control factors on the objective variable. The anode temperature and the anode relative humidity can be identified as the two main parameters affecting the current density. Instead, no clear correlation can be made for relative humidity and temperature at the cathode, neither for compression rate.

The same procedure is adopted for the noise factors. Scatter plots for noise factors are provided in Figure 5. It is quite clear that the most leading parameter is the cathode exchange current density. Moreover, the anode exchange current has more effects than condensation and saturation, and it cannot be neglected. Such behavior is reflected by the Pareto plot shown in the bottom part of Figure 6.

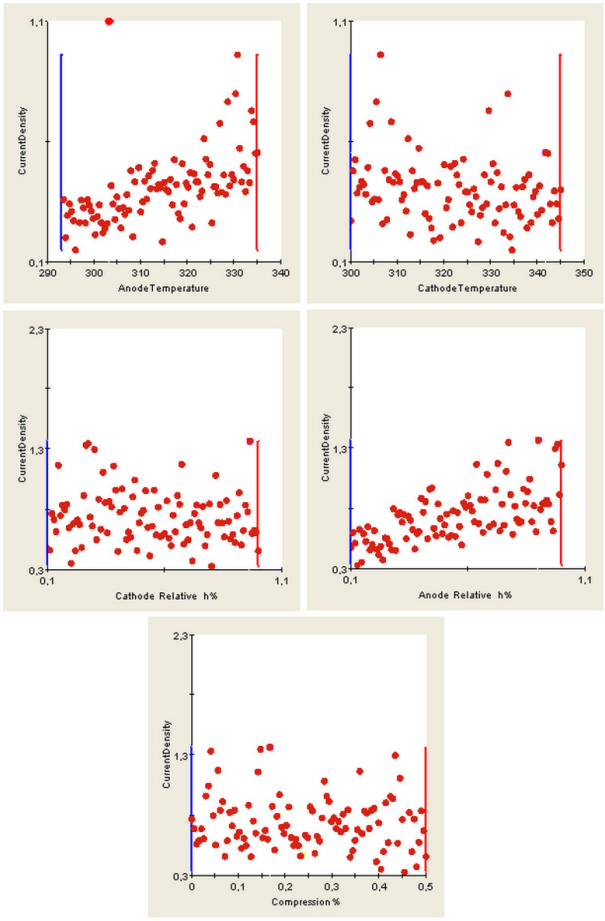

Fig. 4: Scatter plots obtained fort the sensitivity analysis of the control factors. Each red point represents a simulation point of the DoE. For each plot, its corresponding control factor is given in the x-axis, between its lower and upper limits. The objective function is given on the y-axis.

Saturation and condensation rate are instead not directly contributing. At the cathode side the membrane is humidified thanks to the water produced by the electrochemical reaction; the anode usually experiences difficulty in keeping the right membrane humidification, since the presence of liquid water is strictly connected to its transport through the membrane itself and the hydrogen inlet humidification [46, 47].

Despite the membrane is thin, a good amount of membrane humidity must be guaranteed at its two sides, being humidification at only one side not enough. Therefore, the strong importance of humidity at the anode becomes clear. Being the membrane humidification directly proportional to the electric conductivity of the membrane, a higher value of humidification means a higher electric current. This is the reason why it is extremely important to monitor and correctly set the right value of anodic temperature and humidity.

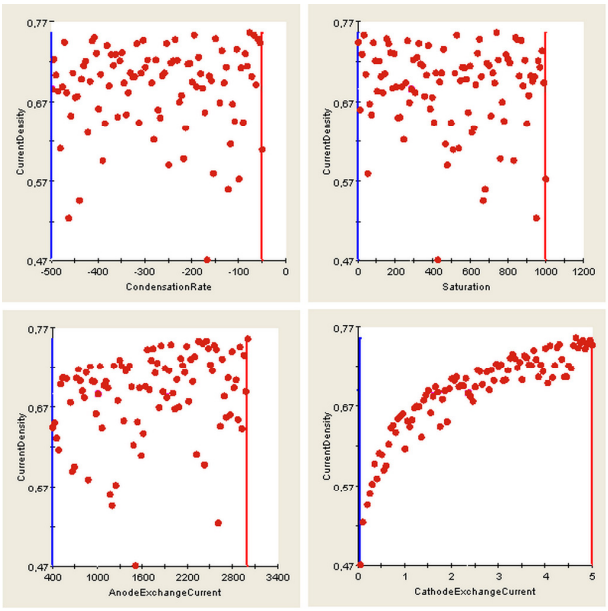

Fig. 5: Scatter plots obtained fort the sensitivity analysis of the noise factors. Each red point represents a simulation point of the DoE. For each plot, its corresponding noise factor is given in the x-axis, between its lower and upper limits. The objective function is given on the y-axis.

The importance of the anode temperature could be justified considering the operating point here simulated, equal to 0.2 V in output. At this low voltage value, the current production is high, meaning a high liquid water production at the cathode side. The back-diffusion of water through the membrane, given by the gradient of concentration at the two sides, is enhanced and can counterbalance the electro-osmotic drag. A lower relative humidity at the anode (i.e. a high inlet temperature) helps in removing the excess water, which could imply water flooding. This behavior is opposed at low or medium current densities, where very high anode relative humidity is always required to prevent the membrane drying. The cathode exchange current density shows a great influence on the polarization curve, being perfectly in-line with the physical explanation already given.

4 Conclusions

The presented work proposes a logic for the evaluation of a PEM FC model behavior and individuates the key factors affecting it. The provided sensitivity analysis is a pivotal input to any MDO process that could be applied to such models, with the aim to reduce computational effort without affecting significantly the representativeness, thus leading to an increase in the efficiency of the model itself. A natural consequence of this activity is the realization of a surrogate model based on the output of this work, aimed to obtain a MDO able to provide and validate the best solution in terms of maximum current density produced at a given voltage. Such objective is going to be achieved through the employment of a Multi-Island Genetic Algorithm, then validated through the comparison of the optimized results from the surrogated model with a simulation of the complete model as a reference of the predicted "real" values.

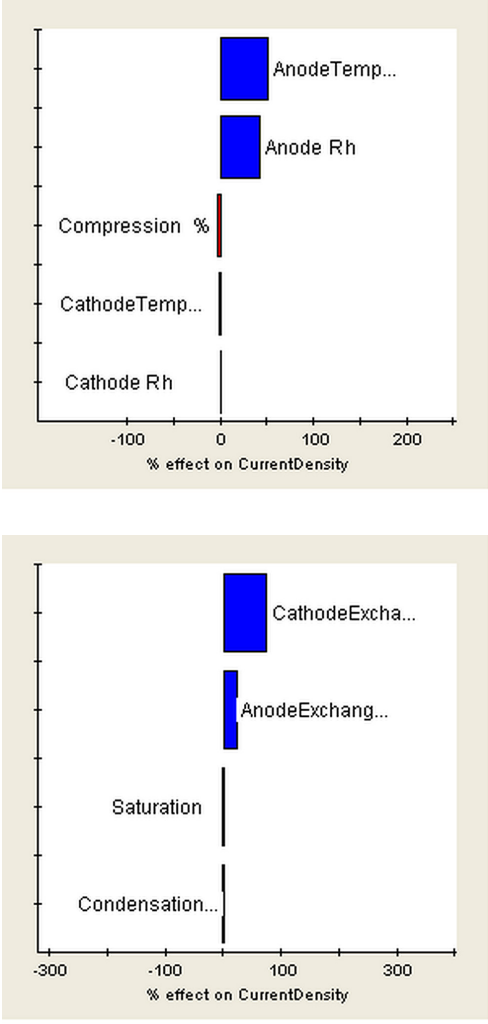

Fig. 6: Pareto plot of the control factors (top), with the noise factors kept to a constant value; Pareto plot of the noise factors (bottom), with the control factors are kept to a constant value. On the x-axis the percentage importance of each control factor on the objective function is shown. Blue colour for positive effects on the objective function and red for negative effects. It is noticeable how the main control factors are temperature and relative humidity at the anode, while the main noise factor is exchange current density both at anode and cathode.

References:

[1] D. M. Bernardi & M. W. Verbrugge. Mathematical model of a gas diffusion electrode bonded to a polymer electrolyte. *AIChE journal*, Vol.37, No.8, 1991, pp. 1151-1163.

[2] S. Dutta, S. Shimpalee & J. W. Van Zee. Three-dimensional numerical simulation of straight channel PEM fuel cells. *Journal of Applied Electrochemistry*, Vol.30, No.2, 2000, pp. 135-146.

[3] S. Dutta, S. Shimpalee & J. W. Van Zee. Numerical prediction of mass-exchange between cathode and anode channels in PEM fuel cell. *Int J Heat and Mass Transf*, Vol.44, 2001, pp. 2029-2042.

[4] T. E. Springer, T. A. Zawodzinski, S. Gottesfled. Polymer electrolyte fuel cell model. *J Electrochem Soc*, Vol.138, 1991, pp. 2334-2342.

[5] K. W. Lum, J. J. McGuirk. Three-dimensional model of a complete polymer electrolyte membrane fuel-cell model formulation, validation and parametric studies. *J Power Sources*, Vol.143, 2005, pp. 103-124. doi: 10.1016/j.jpowsour.2004.11.032

[6] B. R. Sivertsen, N. Djilali N. CFD-based modelling of proton exchange membrane fuel cells. *J Power Sources* Vol.141, 2005, pp. 65-78. doi: 10.1016/j.jpowsour.2004.08.054

[7] A. Z. Weber & J. Newman. Modeling transport in polymer-electrolyte fuel cells. *Chemical Reviews*, Vol.104, No.10, 2004, pp. 4679-4726.

[8] K. Z. Yao, K. Karan, K. B. McAuley, P. Oosthuizen, B. Peppley & T. Xie. A review of mathematical models for hydrogen and direct methanol polymer electrolyte membrane fuel cells. *Fuel Cells*, Vol.4, 2004.

[9] C. Y. Wang. Fundamental models for fuel cell engineering. *Chemical Reviews*, Vol.104, No.10, 2004, pp. 4727-4766.

[10] D. Cheddie & N. Munroe. Review and comparison of approaches to proton exchange membrane fuel cell modeling. *Journal of Power Sources*, Vol.147, 2005, pp. 72-84.

[11] A. Z. Weber et al. A Critical Review of Modeling Transport Phenomena in Polymer-Electrolyte Fuel Cells. *Journal of The Electrochemical Society* Vol.161, No.12, 2014.

[12] G. Panayiotou, P. Axaopoulos, I. Fyrippis. Evaluation and simulation of a commercial 100W Polymer Electrolyte Membrane Fuel Cell (PEMFC) Stack. WSEAS Transactions on Power Systems, Vol.3, No.10, 2008, pp. 633-642.

[13] E. Afshari, S. A. Jazayeri. Heat and Water Management in a PEM Fuel Cell. *WSEAS Transactions on Fluid Mechanics*, Vol.2, No.3, 2008, pp. 137-142.

[14] N. P. Siegel, M. W. Ellis, D. J. Nelson, M. R. Von Spakovsky. A two-dimensional computational model of PEMFC with liquid water transport. *J Power Sources*, Vol.128, 2003, pp.173-184.

[15] M.A.R.S. Al-Baghdadi. A CFD study of hygro-thermal stresses distribution in PEM fuel cell during regular cell operation. *J. Renew Energy*, Vol.34, 2009, pp. 674-682.

[16] D.S. Falcão, P.J. Gomes, V.B. Oliveira, C. Pinho C, A.M.F.R. Pinto. *1D and 3D numerical simulations in PEM fuel cells*. Int J Hydrogen Energy, Vol.36, 2011, pp. 12486-12498.

[17] Z. H. Wang, C.Y. Wang & K.S. Chen. Two-phase flow and transport in the air cathode of proton exchange membrane fuel cells. *Journal of Power Sources*, Vol.94, No.1, 2001, pp. 40-50.

[18] C.Y. Wang & P. Cheng. Multiphase flow and heat transfer in porous media. *Advances in heat transfer*, Vol.30, 1997, pp. 93-196.

[19] S. Um, C.Y. Wang, & K.S. Chen. Computational fluid dynamics modeling of proton exchange membrane fuel cells. *Journal of the Electrochemical society*, Vol.147, No.12, 2000, pp. 4485-4493.

[20] J.E. Dawes, N.S. Hanspal, O.A. Family, A. Turan. Three-dimensional CFD modelling of PEM fuel cells: an investigation into the effects of water flooding. *J Chem Engin Sci*, Vol.64, 2009, pp. 2781-2794. doi: 10.1016/j.ces.2009.01.060.

[21] C.H. Min, Y.L. He, X.L. Liu, B.H. Yin, W. Jiang, W.Q. Tao. *Parameter sensitivity examination and discussion of PEM fuel cell simulation model validation. Part II: results of sensitivity analysis and validation of the model*. J Power Sources, Vol.160, 2006, pp. 374-385. doi: 10.1016/j.jpowsour.2006.01.080

[22] G.H. Guvelioglu H.G. Stenger. Main and interaction effects of PEM fuel cell design parameters. *J Power Sources*, Vol.2, 2005, pp. 424-433. doi: 10.1016/j.jpowsour.2005.06.009

[23] M. Secanell, R. Songprakorp, N. Djilali, A. Suleman. Optimization of a proton exchange membrane fuel cell membrane electrode assembly. *Struct Multidisc Optim*, Vol.40, 2010, pp. 563-583. doi: 10.1007/s00158-009-0387-z

[24] N. Pourmahmoud, S. Rezazadeh, I. Mirzaee, V. Heidarpoor. Three-dimensional numerical analysis of proton exchange membrane fuel cell. *J Mech Sci And Tech*, Vol.25, 2011, pp. 2665-2673. doi: 10.1007/s12206-011-0743-y

[25] N. Ahmadi, S. Rezazadeh, I. Mirzaee, N. Pourmahmoud. *Three-dimensional computational fluid dynamic analysis of the conventional PEM fuel cell and investigation of prominent gas diffusion layers effect*. J Mech Sci And Tech, Vol.26, 2012, pp. 2247-2257. doi: 10.1007/s12206-012-0606-1

[26] C. Kim, H. Sun. Topology optimization of gas flow channel in an automotive fuel cell. *Int J Automot Tech*, Vol.13, 2012, pp. 783-789. doi: 10.1007/s12239−012−0078−4

[27] M. Secanell, J. Wishart, P. Dobson. Computational design and optimization of fuel cells and fuel cell systems: a review. *Journal of Power Sources*, Vol.196, No.8, 2011, pp. 3690-3704.

[28] B. Mukhtar, S. Javaid Zaidi, M. Naim Faqir. Multi-objective function optimization for PEM fuel cell system. *ECS Trans*, Vol.26, 2010, pp. 77-88. doi: 10.1149/1.3428978

[29] R.Y. Rubinstein, D.P. Kroese. *Simulation and the Monte Carlo method* (2nd ed.). John Wiley & Sons, New York, 2007.

[30] K. Deb. *Multi-objective optimization using evolutionary algorithms*. John Wiley & Sons, New York, 2001.

[31] O. Vigna Suria, E. Testa, P. Peraudo, P. Maggiore. A PEM fuel cell distributed parameters model aiming at studying the production of liquid water within the cell during its normal operation: model description, implementation and validation. *In SAE World Congress*, 2011.

[32] ANSYS. *ANSYS FLUENT fuel cell modules manual*. ANSYS, Inc, 2011.

[33] Cao, T. F., Mu, Y. T., Ding, J., Lin, H., He, Y. L., & Tao, W. Q. (2015). Modeling the temperature distribution and performance of a PEM fuel cell with thermal contact resistance. *International Journal of Heat and Mass Transfer*,*87*, 544-556

[34] D3.4.3 *Optimisation and robust design capabilities – achievements, needs and orientations*. CRESCENDO FP7-234344 © Copyright CRESCENDO Consortium, 2009.

[35] A.V. Bernstein, A.P. Kuleshov. Construction of orthogonal non-linear manifolds in the problem of dimension reduction. *Proceedings of 7th International School – Seminar on Multivariate statistical analysis and econometrics*, 2009.

[36] Kahveci, E. E., & Taymaz, I. (2014). Experimental investigation on water and heat management in a PEM fuel cell using response surface methodology. *International Journal of Hydrogen Energy*, Vol.39, pp. 10655-10663

[37] Huang, K. J., Hwang, S. J., & Lai, W. H. (2015). The influence of humidification and temperature differences between inlet gases on water transport through the membrane of a proton exchange membrane fuel cell.*Journal of Power Sources*, Vol.*284*, pp. 77-85

[38] J.F.M. Barthelemy, R.T. Haftka. Approximation concepts for optimum structural design – A review. *Structural Optimization*, Vol.5, 1993, pp. 129-144.

[39] N.A.C. Cressie. *Statistics for spatial data*. John Wiley & Sons, New York, 1993.

[40] M. Papadrakakis, V. Papadapoulos. Robust and efficient methods for stochastic finite element analysis using Monte Carlo simulation. *Computer Methods in Applied Mechanics and Engineering*, Vol.134, 1996, pp. 325-340.

[41] P.N. Peraudo, C. Abbondanza, P. Maggiore. A multi-objective design optimization approach for the preliminary design of high-speed low pressure turbine disks for green engine architectures. *14th Multidisciplinary Analysis and Optimization Conference*, September 2012, Indianapolis, IN. AIAA 2012-5606

[42] B. Tabachnick, G. Fidell, S. Linda. *Using multivariate statistics* (5th ed.). Pearson International Edition, Boston, 2007.

[43] S.M. Stigler. Francis Galton's account of the invention of correlation. *Statistical Science*, Vol.4, 1989, pp. 73-79.

[44] R.K. Ekawati, A.N. Hidayanto. The influence of antecedent factors of IS/IT utilization towards organizational performance: A case study of IAIN Raden Fatah Palembang. *WSEAS Transactions on Computers*, Vol.10, 2011.

[45] D.P. Francis, A.J. Coats, D. Gibson. How high can a correlation coefficient be? Effects of limited reproducibility of common cardiological measures. *Int J Cardiol*, 1999.

[46] Zamel, N., & Li, X. (2013). Effective transport properties for polymer electrolyte membrane fuel cells–with a focus on the gas diffusion layer.*Progress in energy and combustion science*, Vol.39, pp. 111-146.

[47] Chen, L., Cao, T. F., Li, Z. H., He, Y. L., & Tao, W. Q. (2012). Numerical investigation of liquid water distribution in the cathode side of proton exchange membrane fuel cell and its effects on cell performance.I*nternational Journal of Hydrogen Energy*, Vol. 37.